Journal of Power Sources 195 (2010) 3636–3639

Contents lists available at ScienceDirect

Journal of Power Sources

journal homepage: www.elsevier.com/locate/jpowsour

Short communication

Nanochannel arrays as supports for proton exchange membranes in microfluidic fuel cells

Chandelle J. Wadsworth, Naoki Yanagisawa, Debashis Dutta*

Department of Chemistry, University of Wyoming, 1000 East University Avenue, Laramie, WY 82071, United States

ARTICLE INFO

Article history:
Received 24 October 2009
Received in revised form 7 December 2009
Accepted 8 December 2009
Available online 16 December 2009

Keywords:
Microfluidics
Fuel cells
Proton exchange membranes
Sol–gel membranes
Nanochannels

ABSTRACT

In this article, we report the use of nanochannel arrays as supports for proton exchange membranes in microfluidic fuel cells. The proposed design has been demonstrated by fabricating a sodium silicate based sol–gel structure within such an array bridging two microchannels containing the fuel (HCOOH) and the oxidant ($KMnO_4$) streams. A voltage was generated in this system by bringing two platinum electrodes in contact with these solutions and then connecting them through an external circuitry. With this current design, we have been able to generate an open circuit potential of 1.31 V and a maximum current of 31.2 μA at 25 °C.

1. Introduction

The explosive growth of portable and wireless consumer electronics over the past few years has spurred the development of new power source technologies having increased power and energy densities. Although lithium-ion and nickel metal hydride based rechargeable batteries are well serving this requirement at the present, battery technology is unlikely to keep pace with the growing power demands of electronic devices with high broadband applications [1,2]. Further exacerbating the demands on power sources for next generation of personal electronics is the trend towards smaller, lighter and more compact devices. Miniaturized/microfluidic fuel cells have received considerable attention as a promising solution to these demands on portable power sources [3–5]. Fuel cells have the key advantage that the energy is stored in chemical form in the fuel. Therefore, if the conversion platform can be made sufficiently small, and the fuel can be provided in easy to handle, high concentration cartridges, then a fuel cell will provide extended time between recharge for comparably sized rechargeable batteries.

The current state-of-art for microfluidic fuel cells primarily consists of two classes of designs. The first among these does not require a membrane between the cathodic and the anodic compartments but rather relies on the continuous laminar flow of the fuel and oxidant streams within a microchannel to minimize their mixing [6,7]. Although this design tends to yield a high power output due to minimal internal Ohmic resistance, it requires continuous pumping of the fuel and oxidant streams via external means and therefore a supply of external energy. In addition, the need to flow the fuel and oxidant streams at high velocities limits their allowable usage in these devices, which is determined by the residence time of these chemicals in between the electrodes [7]. The other class of designs for microfluidic fuel cells takes a more conventional approach in which an ion-selective membrane is placed between the cathodic and anodic compartments to physically separate the fuel and oxidant streams. Motokawa et al. [8], for example, demonstrated such a device by sealing a commercially available sheet of Nafion membrane between a silicon and glass plate. This design however, although simple to realize, inherently suffered from leakage issues, which in addition to posing potential chemical hazards can also significantly deteriorate its performance due to fuel cross-over. Liu et al. [9] in a different effort described and systematically investigated a new design for microfluidic fuel cells in which sub-micrometer scale channels (nanochannels) fabricated on glass substrates were employed as proton exchange membranes. The selective conductance of protons through the nanochannels was realized in this work by operating the device under electrical double layer overlap conditions. The authors reported that the apparent proton conductivity in the nanochannels under these conditions was several orders of magnitude larger than that in the bulk solution [10]. This design although offered the membrane structure greater mechanical and thermal stability compared to a clamped Nafion sheet, it suffered from a serious practical limitation which was its limited power output (~3 nW). The small amount of

* Corresponding author. Tel.: +1 307 766 4318; fax: +1 307 766 2807.
E-mail address: ddutta@uwyo.edu (D. Dutta).

0378-7753/$ – see front matter © 2010 Elsevier B.V. All rights reserved.
doi:10.1016/j.jpowsour.2009.12.032

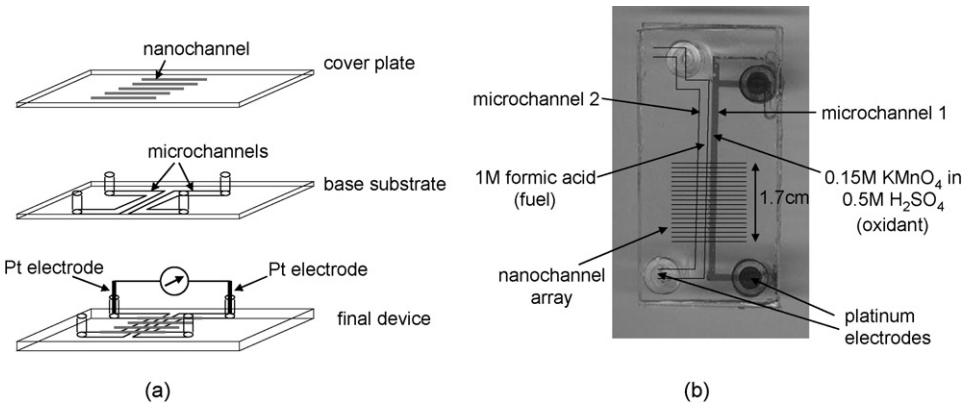

Fig. 1. (a) Schematic of the microfluidic fuel cell design presented in this work. (b) Optical photograph of the microfluidic fuel cell device used in our experiments. The channel containing the fuel stream (formic acid) as well as the array of nanochannels with sol–gel packing structures has been outlined artificially in this picture for clarity.

electrical current that could be drawn out of this device was associated with the small cross-sectional area and substantial length of the nanochannel array that was necessary to minimize fuel cross-over via electroosmotic transport across the anodic and cathodic compartments. More recently, Song et al. [11] presented a PDMS device in which a thin layer of a perfluorinated ion-exchange resin was integrated between two microchannels carrying the fuel and oxidant streams using microfabrication methods. The integrated membrane in this design eliminated all leakage/fuel cross-over issues and allowed a power output that was several orders of magnitude greater than that yielded by Liu et al.'s device.

In this communication, we propose an alternative strategy to creating proton exchange membranes (PEM) for microfluidic fuel cells using a design that employs features from both Liu et al. and Song et al.'s devices. In the proposed design, the PEM is created by selectively retaining a precursor material within a nanochannel array that bridges two microchannels carrying the fuel and the oxidant streams via capillary forces. This precursor is then provided suitable physical/chemical treatment to transform it into an ion-selective membrane. The proposed strategy has been demonstrated in this work by fabricating a sodium silicate based sol–gel structure within a nanochannel array bridging the cathodic and the anodic compartments of a microfluidic fuel cell.

2. Methods and materials

2.1. Device fabrication

The fuel cell device reported in this article comprises two microchannels, 298 μm deep and 1300 μm wide (at half depth), which were chemically etched on a glass substrate using wet etching techniques [12] (see Fig. 1). A second glass plate was then bonded to this substrate using sodium silicate solution (2.7% SiO_2, 1.4% NaOH by weight) as an adhesive layer [13]. Prior to the bonding process however, an array of nanochannels (233 nm deep and 500 μm wide) was chemically etched on the cover plate to accommodate the PEM structure. The bonding between the base substrate and the cover plate was accomplished by first placing excess sodium silicate solution on the cover plate and then immediately bringing the two plates in contact such that the nanochannels etched on the cover plate ran perpendicular to the microchannels created on the base substrate (see Fig. 1). Upon bringing the two plates in contact, the sodium silicate precursor filled up both the microchannels as well as the nanochannel array bridging them. At this point, vacuum was applied to the terminals of the fluidic network to pump out the sodium silicate solution from the microchannels. During this pumping process the solution within the nanochannel bridge did not escape however, due to the larger capillary forces allowing us to selectively retain the precursor material in this region. The device was then treated at 90 °C in a conventional oven at atmospheric pressure for about 15 min to transform the sodium silicate precursor in the nanochannel bridge into a silica gel [13,14], a porous hard glassy substance. Finally, the bonding between the two glass plates was allowed to complete under ambient conditions for about 12 h.

2.2. Device operation

The device described above was operated in our experiments by filling up one of the microchannels with a fuel stream, 1 M formic acid, and the other with an oxidant stream, 0.15 M $KMnO_4$ in 0.5 M H_2SO_4. Upon bringing in contact two platinum electrodes with these solutions in the fluid reservoirs at which the microchannels terminate, an electrical voltage was generated in the system. In this circuitry, the porous silicate structure fabricated within the nanochannel array bridging the two microchannels acted as a PEM that preferentially allowed protons to pass through it [14]. The electrical performance of this fuel cell device was then characterized through open circuit potential and chronoamperometric measurements made using an electrochemical analyzer under different operating conditions.

3. Results and discussion

3.1. Physical characterization of the PEM structure

Prior to the electrical characterization of the microfluidic fuel cell device presented here, efforts were made to visualize the sol–gel membrane structure that was fabricated within a nanochannel array using the procedure described above. In Fig. 2, we have presented an optical image of this membrane created within a nanochannel segment bridging two microchannels that carried the fuel and the oxidant streams. In all our devices, it was observed that the sol–gel structure occupied about 40% of the space in the nanochannel bridge which we believe is likely due to the shrinkage of the sol–gel structure as a result of solvent evaporation during the membrane fabrication process [14]. It was also noted that this sol–gel network sometimes formed at one edge of the nanochannel bridge (as in Fig. 2) and sometimes closer to the center of the nanochannel segment. One reason for this observation may be the statistical nature of the membrane formation process likely initiated by the presence of a glass particle sticking to the channel surface in the nanochannel bridge or the local surface roughness in the nanoscale conduit. In addition, it is also possible that an unequal

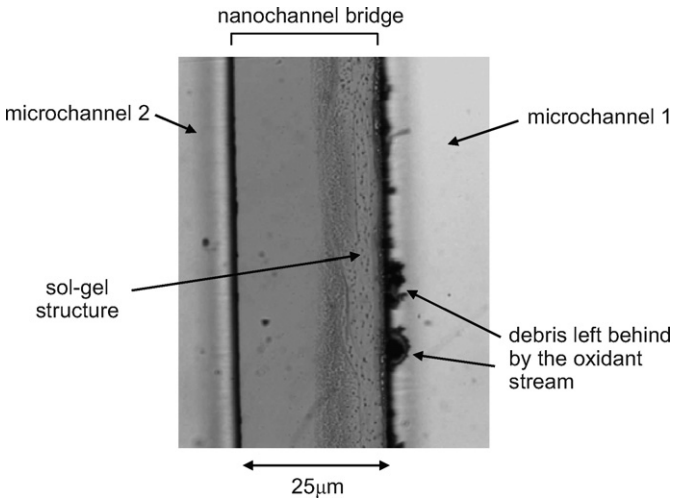

Fig. 2. Optical image of the sodium silicate derived sol–gel membrane fabricated within the nanochannel array of the microfluidic fuel cell device presented in this work.

separation gap between the two glass substrates in the nanochannel bridge at the time of bonding affects the location of the sol–gel membrane. Note that a membrane is more likely to form in a region that has a smaller separation gap as the sodium silicate solution is retained more strongly around this area due to larger capillary forces. It is important to point out however, that the performance of our fuel cell was observed to be unaffected by the location of the sol–gel membrane. The optical image in Fig. 2 also shows that the sol–gel structure formed within the nanochannel bridge was spatially non-uniform.

3.2. Electrical characterization

The electrical performance of the microfluidic fuel cell device described above was characterized in our work by making open circuit potential and chronoamperometric measurements using an electrochemical analyzer (CH Instruments Inc.). In Fig. 3, a typical polarization curve for this device has been presented for an operating temperature of 25 °C. Note that the current density in this figure (the *x*-axis) has been calculated based on the area of the membranes rather than that of the electrodes. This is because no increase in the electrical current was observed in our device when the electrode

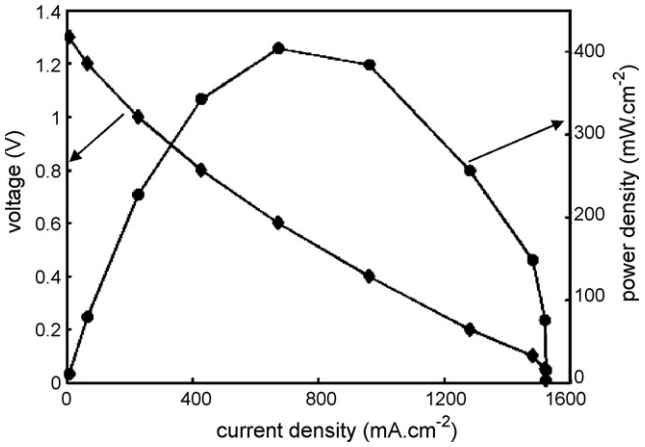

Fig. 3. Polarization curve for the microfluidic fuel cell device presented here when operated at 25 °C. In this experiment a solution of 1 M formic acid was chosen as the fuel while a solution of 0.15 M $KMnO_4$ in 0.5 M sulfuric acid was chosen as the oxidant.

surface area was increased. This suggests that the electrical current delivered by our fuel cell was not limited by the kinetics of the electrochemical reactions but rather by the Ohmic resistance of the membrane, which has also been suggested to be the case for Liu et al.'s [9] device.

Our measurements showed that the open circuit potential for the fuel cell described above was 1.31 V while the maximum current density that could be extracted from it i.e., for a zero external load, was 1487.8 $\mu A\,cm^{-2}$. In this situation, the maximum power output of this unit was calculated to be 405.3 $\mu W\,cm^{-2}$. These numbers correspond to a maximum total current of 31.2 μA and a maximum total power of 8.5 μW. If the maximum current and power densities were calculated based on the surface area of the electrodes in our device, these quantities turn out to be 49.7 $\mu A\,cm^{-2}$ and 13.5 $\mu W\,cm^{-2}$, respectively. Note that because current densities of the order of 1 $mA\,cm^{-2}$ or higher have been reported in the literature [4] for the choice of fuel, oxidant and catalyst used in this work, the hypothesis that the power output of our device was not limited by the surface area of the electrodes is further supported.

The observed power output of our device corresponds to an improvement in this quantity by a factor of 2833 (8.5 μW versus 3 nW) over that reported for the fuel cell design presented by Liu et al. [9] We believe that this improvement is primarily accomplished due to the use of a low resistance PEM structure in our system. The presence of this structure allows us to use a high concentration of fuel and oxidant in our device enhancing the kinetics of the electrochemical reactions as well as minimizing the internal Ohmic resistance of the fuel cell. Note that in the case of Liu et al.'s device, a high concentration of the fuel and oxidant may not have been permissible in order to realize the electrical Debye layer overlap condition within the nanochannels that was necessary for the operation of their fuel cell. It is also interesting to note that the total electrical current output of our device was observed to be 8 times higher than that reported by Song et al. (31.2 μA versus 4 μA) [11] although the fuel concentration used in that work was about 8 times greater than that used in our experiments. In addition, the open circuit potential reported by Song et al. was about 40% lower than that observed for our fuel cell. While the larger current output in our device may be associated with the lower Ohmic resistance of our PEM, we believe that the quality of the electrodes (external electrodes in our case versus micropatterned electrodes in Song et al.'s device) may have determined the difference in the open circuit potential measurements. In any case, these findings suggest that the use of micropatterned electrodes, which requires a greater fabrication effort, may not be necessary in a microfluidic fuel cell design with an integrated PEM.

In Fig. 4, we have depicted the effect of temperature and fuel/oxidant concentrations on the performance of our microfluidic fuel cell device. Fig. 4(a) shows that upon increasing the operating temperature, greater electrical power could be extracted out of the microfluidic fuel cell presented here. For example, the maximum current density that can be drawn out of our device increases from 1487.8 $\mu A\,cm^{-2}$ to 1955.2 $\mu A\,cm^{-2}$ upon increasing the operating temperature from 25 °C to 70 °C. The same increase in temperature however, was not observed to significantly affect the open circuit potential in the system. In these experiments, the operating temperature of our fuel cell was controlled by placing the device on a hot plate. In Fig. 4(b) we have presented the effect of fuel/oxidant concentrations on the performance of our device. As may be seen from the figure, a reduction in the concentration of the fuel or the oxidant used reduces the power output of our fuel cell. Again, we believe that the observed increase in power output with an increase in operating temperature or fuel/oxidant concentrations is likely due to an increased conductance of our membranes rather than any enhancement in the reaction kinetics.

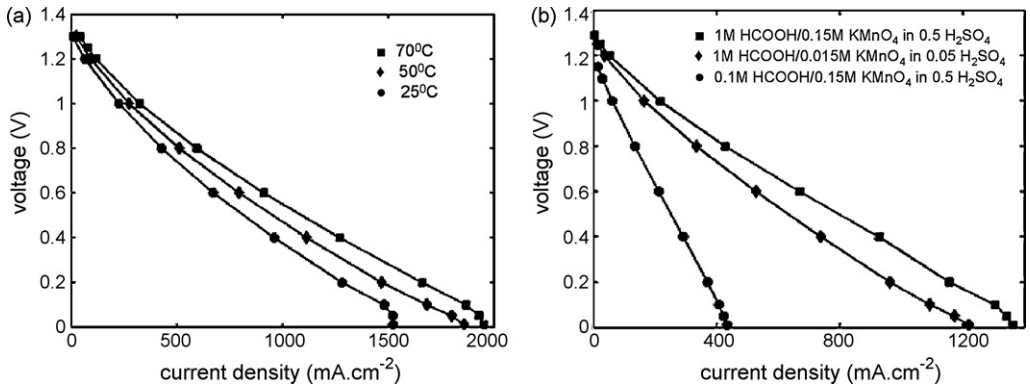

Fig. 4. (a) Effect of operating temperature on the performance of the microfluidic fuel cell device presented in this work when operated with a 1 M formic acid fuel stream and 0.15 M $KMnO_4$ in 0.5 H_2SO_4 oxidant stream. (b) Effect of fuel and oxidant concentrations on the performance of microfluidic fuel cell presented in this article when operated at 25 °C.

Finally, we would like to point that the choice of the oxidant ($KMnO_4$) in our experiments was not the best one as it led to the deposition of brown debris (likely to be MnO_2 particles) around the sol–gel membrane (see Fig. 2). Although this deposition did not appear to affect the performance of the fuel cell in our experiments, we suspect this problem could significantly shorten the life time of our device. Interestingly, these debris could be completely cleaned out from the microchannels in our device by rinsing them with a solution of 90% 0.5 M H_2SO_4 and 10% H_2O_2 for about 10 min. In this work, adopting the above described rinsing procedure after every experimental run may have allowed us to use our microfluidic fuel cell for multiple experiments without noticing any deterioration in its performance. In a real application however, the problem of membrane fouling by $KMnO_4$ may be more easily addressed by simply switching to a different oxidant system, e.g., hydrogen peroxide [15]. The only reason we had chosen to use $KMnO_4$ in our experiments was to be able to directly compare the performance of our fuel cell device to those presented by Liu et al. [9] and Song et al. [11].

4. Conclusions

To conclude, we have demonstrated a novel microfluidic fuel cell device that employs a sodium silicate based sol–gel structure supported within a nanochannel array as the proton exchange membrane (PEM). Experiments show that this architecture allows an enhancement in the power output by a factor of 2833 over a similar device that employs an open nanochannel array as the PEM. Moreover, the proposed design yields a maximum current that is 8 times higher than that produced by a similar device with an integrated perfluorinated ion-exchange membrane. It is also to be noted that the fabrication effort involved in creating the PEM structure in this work is significantly less than that reported by Song et al. [11] which is likely to reduce the manufacturing cost of these devices. It is anticipated that production of the proposed fuel cells to be no more expensive than that of any other glass microfluidic device. However, with advancements in nanofabrication techniques, it may be possible to adopt this technology to polymer/ceramic based devices which could significantly cut down the manufacturing cost when produced on a large scale. Finally, it is important to point out that while the membrane in this work was fabricated using a sodium silicate precursor, the proposed device could potentially accommodate PEMs made out of other materials offering flexibility to our fuel cell design.

Acknowledgements

This research was supported by a grant from the Wyoming NASA Space Grant Consortium, Grant #NNG05G165H, and start-up funds from the University of Wyoming.

References

[1] C.K. Dyer, J. Power Sources 106 (2002) 31–34.
[2] D. Ilic, K. Holl, P. Birke, T. Wöhrle, F. Birke-Salam, A. Perner, P. Haug, J. Power Sources 155 (2006) 72–76.
[3] A. Heinzel, C. Hebling, M. Müller, M. Zedda, C. Müller, J. Power Sources 105 (2002) 250–255.
[4] E. Kjeang, N. Djilali, D. Sinton, J. Power Sources 186 (2009) 353–369.
[5] S. Pennathur, J.C.T. Eijkel, A. van den Berg, Lab Chip 7 (2007) 1234–1237.
[6] R. Ferrigno, A.D. Stroock, T.D. Clark, M. Mayer, G.M. Whitesides, J. Am. Chem. Soc. 124 (2002) 12930–12931.
[7] E.R. Choban, L.J. Markoski, A. Wieckowski, P.J.A. Kenis, J. Power Sources 128 (2004) 54–60.
[8] S. Motokawa, M. Mohamedi, T. Momma, S. Shoji, T. Osaka, Electrochem. Commun. 6 (2004) 562–565.
[9] S. Liu, Q. Pu, L. Gao, C. Korzeniewski, C. Matzke, Nano Lett. 5 (2005) 1389–1393.
[10] D. Stein, M. Kruithof, C. Dekker, Surface charge governed ion transport in nanofluidic channels, Phys. Rev. Lett. 93 (2004) (Art. No. 035901).
[11] Y. Song, C. Batista, R. Sarpeshkar, J. Han, J. Power Sources 183 (2008) 674–677.
[12] D.R. Reyes, D. Iossifidis, P.A. Auroux, A. Manz, Anal. Chem. 74 (2002) 2623–2636.
[13] H.Y. Wang, R.S. Foote, S.C. Jacobson, J.H. Schneibel, J.M. Ramsey, Sens. Actuators B 45 (1997) 199–207.
[14] R. O'Hayre, S.K. Cha, W. Colella, F.B. Prinz, Fuel Cell Fundamentals, John Wiley & Sons, New York, 2006.
[15] E. Kjeang, A.G. Brolo, D.A. Harrington, N. Djilali, D. Sinton, J. Electrochem. Soc. 154 (2007) B1220–B1226.